ASTRONOMY

Primordial formation of major silicates in a protoplanetary disc with homogeneous $^{26}Al/^{27}Al$

Timothy Gregory[1,2,3]*, Tu-Han Luu[1], Christopher D. Coath[1], Sara S. Russell[2], Tim Elliott[1]

Understanding the spatial variability of initial $^{26}Al/^{27}Al$ in the solar system, i.e., $(^{26}Al/^{27}Al)_0$, is of prime importance to meteorite chronology, planetary heat production, and protoplanetary disc mixing dynamics. The $(^{26}Al/^{27}Al)_0$ of calcium-aluminum–rich inclusions (CAIs) in primitive meteorites (~5×10^{-5}) is frequently assumed to reflect the $(^{26}Al/^{27}Al)_0$ of the entire protoplanetary disc, and predicts its initial $^{26}Mg/^{24}Mg$ to be ~35 parts per million (ppm) less radiogenic than modern Earth (i.e., $\Delta'^{26}Mg_0 = -35$ ppm). Others argue for spatially heterogeneous $(^{26}Al/^{27}Al)_0$, where the source reservoirs of most primitive meteorite components have lower $(^{26}Al/^{27}Al)_0$ at ~2.7×10^{-5} and $\Delta'^{26}Mg_0$ of −16 ppm. We measured the magnesium isotope compositions of primitive meteoritic olivine, which originated outside of the CAI-forming reservoir(s), and report five grains whose $\Delta'^{26}Mg_0$ are within uncertainty of −35 ppm. Our data thus affirm a model of a largely homogeneous protoplanetary disc with $(^{26}Al/^{27}Al)_0$ of ~5×10^{-5}, supporting the accuracy of the $^{26}Al \rightarrow ^{26}Mg$ chronometer.

INTRODUCTION

The discovery of correlated $^{26}Mg/^{24}Mg$ with Al/Mg in refractory inclusions in primitive meteorites (*1*)—chondrites—bore witness to the previous presence of live ^{26}Al ($^{26}Al \rightarrow ^{26}Mg$; $t_{1/2}$ = ~0.730 million years (Ma); see the Supplementary Materials) in the nascent solar system, in abundances sufficient to drive melting and metamorphism in planetesimals (*2*), and provide a valuable high-resolution chronometer of early solar system processes (*2*, *3*). Moreover, the inferred $(^{26}Al/^{27}Al)_0$ was sufficiently high to place important constraints on the birth environment of the solar system and the processes that mixed recently synthesized nuclides into the pre-solar nebula and protoplanetary disc [see (*4*)].

Solar system $(^{26}Al/^{27}Al)_0$ has largely been derived from analyses of "normal" calcium-aluminum–rich inclusions (CAIs): ultrarefractory condensates found in unequilibrated chondrites that are the oldest dated objects in the solar system (*5*, *6*), and whose age, with a weighted mean of 4567.30 ± 0.16 Ma, is commonly taken to represent "time zero" of solar system history. Their antiquity and high elemental Al/Mg ratios enable precise determination of $(^{26}Al/^{27}Al)_0$. These works (*7*–*9*) have yielded a canonical $(^{26}Al/^{27}Al)_0$ of ~5.3×10^{-5} that is frequently assumed to reflect the $(^{26}Al/^{27}Al)_0$ of the solar system as a whole.

Canonical $(^{26}Al/^{27}Al)_0$ is one order of magnitude higher than the galactic background, as measured by γ-ray spectroscopy (*10*), indicating that ^{26}Al was injected into the nascent solar system from its stellar source (*11*) shortly before or just after the formation of the protoplanetary disc. This may not have allowed sufficient time for ^{26}Al to be spatially homogenized before the CAIs formed. Heterogeneity in solar system $(^{26}Al/^{27}Al)_0$ is evident in some rare refractory objects (*12*)—namely, some FUN (fractionation and unidentified nuclear isotope effects) CAIs (*13*), BAGs (blue aggregates), and PLACs (platy crustal fragments) (*14*)—which contain no evidence for live ^{26}Al. This observation is commonly interpreted to indicate that these inclusions formed before ^{26}Al was injected into the protoplanetary disc (*15*). These unusual objects preserve an interesting window into early solar system mixing, but we believe are not representative of the bulk of material in the protostellar disc. In this study, we focus only on the solar system's evolution after the condensation of normal CAIs.

Nonetheless, even normal CAIs (hereafter referred to as CAIs) are demonstrably anomalous in their isotopic compositions of many elements relative to the material that comprises bulk meteorites and the terrestrial planets (*16*, *17*). It is therefore reasonable to question whether $(^{26}Al/^{27}Al)_0$ determined from CAIs is representative of the solar system as a whole. Spatially heterogeneous $(^{26}Al/^{27}Al)_0$ within the protoplanetary disc would compromise the utility of the $^{26}Al \rightarrow ^{26}Mg$ decay system for dating early solar system processes, as Al-Mg chronometry traditionally assumes the same $(^{26}Al/^{27}Al)_0$ in CAIs and the object being dated. Much of the understanding of early solar system chronology was developed from the Al-Mg chronometer, so assessing the robustness of its underlying assumptions is of paramount importance. Previous attempts to assess spatial $(^{26}Al/^{27}Al)_0$ homogeneity using concordance between Al-Mg and other radioisotope chronometers have yielded conflicting conclusions (*18*–*21*).

Consequently, there has been much interest in trying to establish independent constraints on whether or not $(^{26}Al/^{27}Al)_0$ was spatially homogeneous in the protoplanetary disc. An important perspective is provided by the evolution of the radiogenic daughter isotope ratio, $^{26}Mg/^{24}Mg$, with time. For $(^{26}Al/^{27}Al)_0 = 5.32 \times 10^{-5}$ (*8*), the initial solar system $^{26}Mg/^{24}Mg$, expressed in linearized delta notation as $\Delta'^{26}Mg_0$ [see (*22*) and the Supplementary Materials], should be −34.7 ± 1.4 ppm in order for chondritic meteorite reservoirs to evolve to their modern compositions (Fig. 1). We refer to this as the "canonical model."

The most recent, highest-precision analyses of bulk refractory inclusions in chondrites define an isochron slope in keeping with previous studies, $(^{26}Al/^{27}Al)_0$ of (5.26 ± 0.01) × 10^{-5}, but $\Delta'^{26}Mg_0$ of −15.8 ± 1.2 ppm (*9*); this initial $\Delta'^{26}Mg_0$ implies that bulk CI chondrites (Ivuna-like carbonaceous chondrites, which are the chondrite group thought to best represent the bulk solar system composition) had a reduced $(^{26}Al/^{27}Al)_0$ of (2.71 ± 0.21) × 10^{-5} to evolve to their modern $\Delta'^{26}Mg$ (Fig. 1). Calculations of $(^{26}Al/^{27}Al)_0$ for bulk ordinary and bulk enstatite chondrites based on their modern $\Delta'^{26}Mg$ and $^{27}Al/^{24}Mg$, assuming that they each had $\Delta'^{26}Mg_0$ of −15.8 ppm (fig. S1), also yield

[1]School of Earth Sciences, University of Bristol, Wills Memorial Building, Bristol BS8 1RJ, UK. [2]Department of Earth Sciences, The Natural History Museum, Cromwell Road, London SW7 5BD, UK. [3]National Environmental Isotope Facility, British Geological Survey, Nottingham NG12 5GG, UK.
*Corresponding author. Email: timothy.gregory@bristol.ac.uk

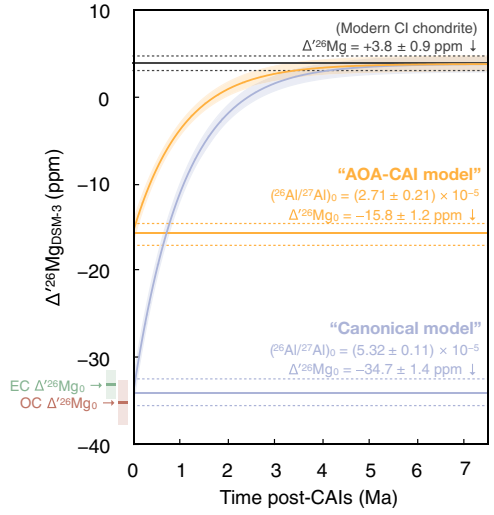

Fig. 1. Illustration of two $\Delta'^{26}Mg$ evolution models for chondrite parent bodies. The canonical model (purple curve), consistent with widespread $(^{26}Al/^{27}Al)_0$ homogeneity, uses the modern composition of CI chondrites (*9*, *37*, *47*) and $(^{26}Al/^{27}Al)_0$ of $(5.32 \pm 0.11) \times 10^{-5}$ (*8*, *9*) to yield $\Delta'^{26}Mg_0 = -34.7 \pm 1.4$ ppm. Ordinary chondrites (OC) and enstatite chondrites (EC), two major classes of chondrites, yield statistically identical $\Delta'^{26}Mg_0$ based on their modern compositions (*9*, *37*, *47*). (ii) The alternative "AOA-CAI" model (orange curve) assumes $\Delta'^{26}Mg_0$ of −15.8 ppm (*9*), consequently requiring $(^{26}Al/^{27}Al)_0$ a factor of ~2 lower than the canonical model to evolve to modern CI composition, reflecting $(^{26}Al/^{27}Al)_0$ heterogeneity between the portion of the protoplanetary disc that condensed CAIs and that which contributed to bulk chondrites. Uncertainty bars/areas are ±2 SE.

similarly subcanonical $(^{26}Al/^{27}Al)_0$. These observations seemingly provide evidence for differences in $(^{26}Al/^{27}Al)_0$ between the portion of the protoplanetary disc that condensed CAIs and that which contributed to the bulk chondrites and, by inference, the reservoir for the terrestrial planets.

If this is the case, the key assumption of spatial $(^{26}Al/^{27}Al)_0$ homogeneity is invalid, and a substantial reinterpretation of Al-Mg chronometry of early solar system objects is required (*19*). Yet, the use of so-called amoeboid olivine aggregates [AOAs: aggregates of forsteritic olivine with an oxygen isotopic composition similar to CAIs (*23*)] alongside CAIs in the construction of the isochron that yields the intercept $\Delta'^{26}Mg_0$ of −15.8 ppm (*9*) has been a matter of considerable debate as the AOAs strongly influence the value of the intercept, but the temporal and genetic relationship between CAIs and AOAs is still unclear (*24*). Hence, we refer to the model with lower bulk chondritic $(^{26}Al/^{27}Al)_0$, deduced from the isochron of (*9*), as the "AOA-CAI model" (Fig. 1).

To provide a new perspective on this debate, we have probed the evolution of $\Delta'^{26}Mg$ in individual olivine grains from primitive meteorites. These low-Al/Mg minerals require minimal correction to obtain their $\Delta'^{26}Mg_0$, unlike CAIs, for which measured $\Delta'^{26}Mg$ requires considerable extrapolation (and associated uncertainty) to return $\Delta'^{26}Mg_0$. Our target grains have a typical $^{27}Al/^{24}Mg$ of 4×10^{-3} (see Results), and so, even with a CAI-like $(^{26}Al/^{27}Al)_0$ of 5.3×10^{-5}, the ingrowth of radiogenic ^{26}Mg (i.e., ^{26}Mg derived from the decay of ^{26}Al) would only increase $\Delta'^{26}Mg$ by ~1.5 ppm. This is negligible compared to the typical precision of our isotope analyses (~3 ppm) and the differences between the $\Delta'^{26}Mg$ we are trying to resolve. We assume the measured $\Delta'^{26}Mg$ of the olivines to represent their $\Delta'^{26}Mg_0$. In the most straightforward case, if an olivine yields $\Delta'^{26}Mg_0$ significantly lower than −15.8 ± 1.2 ppm, this rules out the AOA-CAI model. At the same time, we would anticipate no values less than −34.7 ± 1.4 ppm if the canonical model is correct.

A challenge for this crucial test is to identify for analysis sufficiently old olivine that formed outside of the CAI-forming reservoir(s). Given that $\Delta'^{26}Mg$ can routinely be measured at the University of Bristol to a precision of ±5.0 ppm (2 SE) for the small amounts of magnesium available in individual olivine grains (typically <5 μg for an olivine grain of ~200 μm), we can only differentiate olivines that have formed before the two modeled curves converge to within ~5.0 ppm of one another. This corresponds to a time of formation no later than ~1.4 Ma after CAIs.

Previously, the magnesium isotope evolution of the early solar system has been investigated using in situ measurements of olivine dated in chondrules (*25*)—quenched melt droplets that formed in the protoplanetary disc that are the dominant component of primitive meteorites (*26*)—but these grains were too young, given the precision of analysis, to resolve the two scenarios illustrated in Fig. 1 (see also fig. S1). Rather than analyze typical chondrule olivine, here, we target refractory forsterite grains (RFs) in unequilibrated carbonaceous chondrites. RFs are volumetrically minor (*27*) but ubiquitous in unequilibrated chondrites occurring in three petrographic settings: as (i) isolated grains in chondrite matrix that formed via fragmentation of preexisting chondrules (*28*), (ii) in situ phenocrysts in magnesium-rich ("type I") chondrules (*27*) (Fig. 2), and (iii) so-called relict grains in the cores of olivine phenocrysts in iron-rich ("type II") chondrules, which represent unmolten chondrule precursors (*29*). The eponymous feature of these grains is their high-Mg/(Mg + Fe) and relatively high, but still trace, concentrations of refractory elements Al, Ti, and Ca in their structure compared to more common meteoritic olivine (*30*). These characteristics are compatible with their formation at an early stage of disc evolution in high-temperature, low-fO_2 conditions (*31*). Moreover, their petrographic relationships with later-formed silicates (*29*), namely, their presence as "relict" grains in some type II chondrules, show that they predate at least some chondrules. So, although they are not absolutely dated, RFs are demonstrably older than at least some chondrules and therefore preserve isotopic information from the solar system's earliest history.

RESULTS

The refractory nature of RFs is evident in their highly forsteritic compositions ($Fo_{>98.5}$) and elevated refractory element contents compared to most chondrule olivine and also AOAs (Fig. 3A). With $\Delta'^{17}O$ (mass-independent oxygen isotope composition; see the Supplementary Materials) of ~−5.6‰, they are ^{16}O poor compared to CAIs and AOAs (Fig. 3B) but are similar to bulk chondrules from carbonaceous chondrites (*32*).

RFs have $\Delta'^{26}Mg_0$ ranging from 8.1 ± 2.7 to −40.2 ± 16.9 ppm (Fig. 3C). Critically, 4 (of 13) of our RFs have $\Delta'^{26}Mg_0$ values that are significantly lower than the lowest possible $\Delta'^{26}Mg_0$ of −15.8 ± 1.2 ppm of the AOA-CAI model (*9*), while none are lower than the lowest possible $\Delta'^{26}Mg_0$ of −34.7 ± 1.4 ppm of the canonical model (Fig. 3C). Because of the low Al/Mg of these objects, this holds true even if the minor amount of ^{26}Mg ingrowth is corrected for. The $\Delta'^{26}Mg_0$ model ages of RFs, calculated relative to the $\Delta'^{26}Mg$ evolution curve (Fig. 1), range from −0.14 ± 0.40 to >4 Ma after CAIs (Fig. 4A). The oldest RFs (i.e., lowest $\Delta'^{26}Mg_0$) all have high refractory element concentrations (Fig. 3, C and D), whereas, in the younger samples, refractory element abundances decrease to those of more typical chondrule olivines.

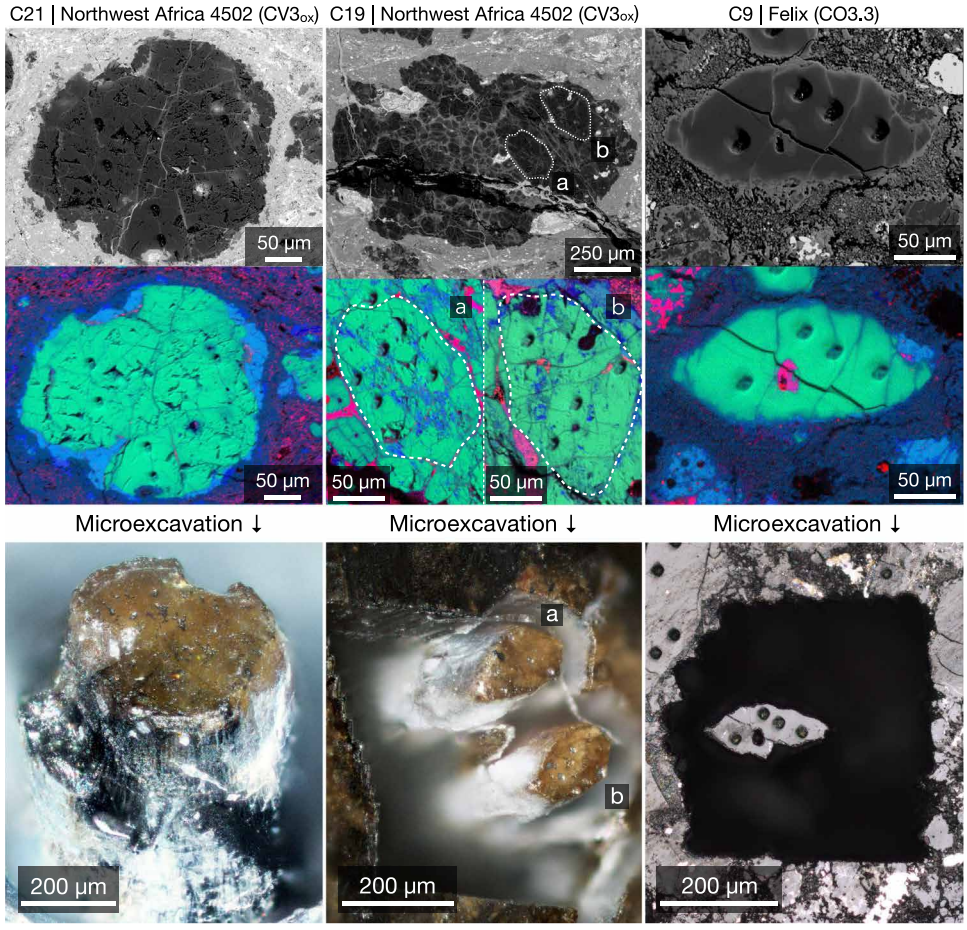

Fig. 2. Examples of RFs as isolated matrix grains (left and right) and in situ phenocrysts in a magnesium-rich (type I) chondrule (middle, dashed outlines). Careful high-resolution microexcavation of material adjacent to RFs before microsampling (bottom panels; see also the Supplementary Materials) reduces the risk of inadvertently sampling unwanted neighboring material. Top panels are backscattered electron maps, middle panels are K_α x-ray maps (green, magnesium; blue, silicon; red, aluminum; green, olivine; light-blue, pyroxene; pink/red, Al-rich phases), and bottom panels are optical images.

DISCUSSION

While there is oxygen isotope heterogeneity among CAIs, the majority from the least equilibrated (i.e., most petrologically pristine) chondrites have isotopically uniform $\Delta'^{17}O$ at ~−24‰, likely reflecting the composition of their source reservoir(s) (*33*). Chondrules have a range in $\Delta'^{17}O$, clustering between $\Delta'^{17}O$ of ~−8‰ and +2‰. It is therefore reasonable to use the $\Delta'^{17}O$ of RFs to genetically link them with the chondrule-forming region(s) and distinguish them from the region(s) of the solar system that condensed CAIs. Although $\Delta'^{17}O$ variability is commonly argued to result from photochemical reactions within the solar system (*34*), meteorites show covariations of $\Delta'^{17}O$ with a range of mass-independent isotope anomalies that reflect variable inputs from different stellar sources (*35*). Why isotopic anomalies with such different origins covary is not well understood, but empirically, $\Delta'^{17}O$ is a good proxy for heterogeneous distribution of pre-solar material in the nebula. The $\Delta'^{17}O$ measurements of our RFs link them to the reservoir of material that formed the major silicate component of chondrites, including chondrules (Fig. 3B).

The idea that four RFs have $\Delta'^{26}Mg_0$ lower than the lowest possible value predicted by the "CAI-AOA model" argues against this model's general applicability and strengthens concerns that inclusion of AOAs and CAIs on the same isochron is ill advised. Rather, these four most unradiogenic RFs have $\Delta'^{26}Mg_0$ within uncertainty of −34.7 ± 1.4 ppm, the value for the solar system at the onset of CAI formation, as calculated using canonical $(^{26}Al/^{27}Al)_0$ for CI chondrites (Fig. 1). Because no RF has $\Delta'^{26}Mg_0$ significantly lower than this "canonical" value, it seems unlikely that their distinctive magnesium isotopic compositions are of a nucleosynthetic origin (i.e., isotope anomalies inherited from heterogeneously distributed pre-solar carriers). While possible in principle, it would seem implausibly serendipitous for these nucleosynthetic compositions to fit exactly in the small window predicted by independently constrained radiogenic decay.

Previously, a positive array of correlating ^{26}Mg and ^{54}Cr anomalies in bulk meteorites and CAIs (*9*, *36*) was argued to track coupled heterogeneous distribution of $(^{26}Al/^{27}Al)_0$ and stable nucleosynthetic anomalies in the protoplanetary disc. The purported correlation was strongly pinned by a model $\Delta'^{26}Mg_0$ for the "CAI-AOA reservoir," derived from the intercept of the CAI-AOA isochron (*9*). As discussed above, our measurements argue against the validity of this value. Moreover, subsequent work on bulk chondrites has illustrated that their variable $\Delta'^{26}Mg$ can be explained by their variable Al/Mg from a common canonical initial $\Delta'^{26}Mg$ and $^{26}Al/^{27}Al$ (*37*, *38*). Thus, the arguments made in (*9*) appear no longer relevant. It has become

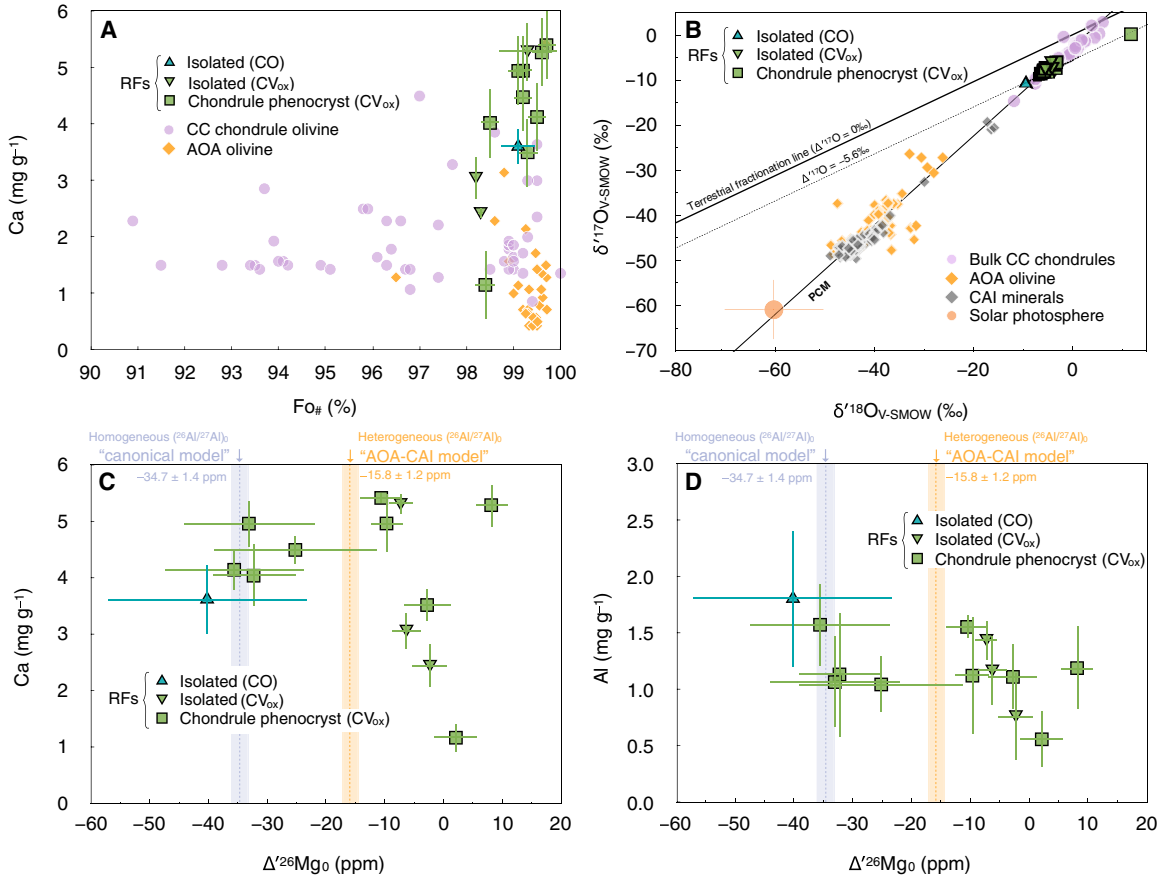

Fig. 3. The chemical and isotopic compositions of RFs compared to CAIs, AOAs, chondrules, and both Δ'^{26}Mg evolution models. (**A**) RFs ($Fo_{>98.5}$) are Ca-rich relative to AOAs and CAIs. (**B**) Oxygen isotope compositions similar to bulk carbonaceous chondrite (CC) chondrules distinguish RFs from AOAs and CAIs, linking them to the major silicates in chondrites. We show the primitive chondrule mineral (PCM) line (*48*), the terrestrial fractionation line, and a fractionation line at $\Delta'^{17}O = -5.6‰$ around which our RF data cluster. Measured $\Delta'^{26}Mg_0$ of RFs relative to the end-member $\Delta'^{26}Mg_0$ models (vertical bars) plotted against (**C**) calcium and (**D**) aluminum concentrations. Four RFs are well resolved from the AOA-CAI model. All uncertainties are ±2 SE (omitted on literature data and smaller than symbols for our oxygen data). Literature references are given in the Supplementary Materials.

apparent that Renazzo-like 'CR' chondrites are anomalous in their magnesium isotopic compositions relative to other chondrites, but this has been widely ascribed to magnesium isotope heterogeneity in an isolated part of the disc (*36*), rather than differences in their $(^{26}Al/^{27}Al)_0$.

Thus, our data provide valuable new support for the previous assumption of a spatially homogeneous $(^{26}Al/^{27}Al)_0$ between the CAI and the main chondrite-forming reservoirs of the protoplanetary disc. Given that CAIs likely formed in close proximity to the young Sun (*39*) and carbonaceous chondrites likely hail from bodies that formed in the outer solar system before being scattered into their current positions in the asteroid belt (*40*), this is compelling evidence for widespread well-mixed and homogeneous $(^{26}Al/^{27}Al)_0$ across much of the early solar system. A homogeneous $(^{26}Al/^{27}Al)_0$ of ~5.3×10^{-5} returns $\Delta'^{26}Mg_0$, consistent with the canonical model for the other major classes of chondrites (ordinary and enstatite chondrites; Fig. 1 and fig. S1), extending the $(^{26}Al/^{27}Al)_0$ homogeneity to the formation reservoirs of diverse classes of chondrites.

The similarity of RFs to chondrules in terms of their oxygen isotope compositions, and their presence as large phenocrysts in type I chondrules, suggests that RFs are the products of crystallization from parental melts—i.e., they are the products of crystallization of chondrule-like objects—rather than direct gas-solid condensates. This is consistent with the view that RFs crystallized from condensed silicate melts at high-temperature and low-fO_2 conditions (*27*). Therefore, one interpretation of the model ages of RFs is that they represent the crystallization of refractory element–rich condensed melts (i.e., refractory element–rich chondrule-forming events).

The range in model ages of RFs indicates either a protracted period of formation over ~4 Ma or early formation followed by variable reequilibration with an evolving nebula. This latter notion is in keeping with ideas of continued chondrule reprocessing and interaction with nebula gas [e.g., (*41*)]. The continuum of RF $\Delta'^{26}Mg$ model ages from values as old as CAIs to several Ma younger is consistent with single-chondrule Pb-Pb ages (*6*, *42*) but contrasts with the marked peak in relatively young ages for internal Al-Mg isochrons for single chondrules (Fig. 4, B and C). We attribute the ~2 Ma offset between Al-Mg ages of CAIs and chondrules, evident in literature data, to the effects of transient thermal events (*43*) in the protoplanetary disc that reset Al-Mg internal isochrons but incompletely reset the Pb-Pb chronometer. We suggest that these thermal events largely ceased ~2 to 3 Ma after CAIs, resulting in most chondrules recording this age in their internal Al-Mg ages. Most internal Al-Mg isochrons of chondrules are pinned by high-Al/Mg phases [e.g., small plagioclase (<20 μm) or microcrystalline mesostasis], which are both more fusable

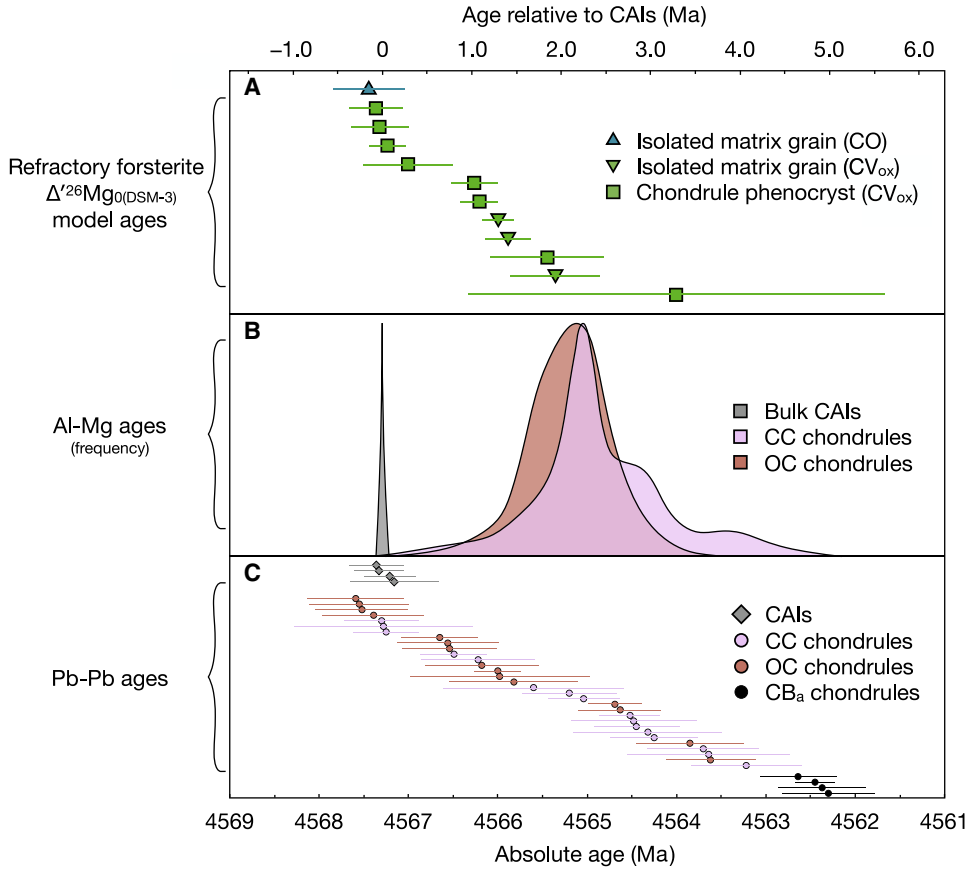

Fig. 4. The onset of the solar system's rock record as recorded by Al-Mg and Pb-Pb systematics in chondrites. (**A**) Magnesium $\Delta'^{26}Mg_0$ model ages of RFs (this study), which span from CAI formation (time zero) to ~3 to 4 Ma. (**B**) Kernel density estimate curves of Al-Mg bulk CAIs and internal chondrule ages (literature sources; see the Supplementary Materials), showing a well-defined CAI peak and a broad chondrule peak ~2 to 3 Ma later. (**C**) Pb-Pb ages of individual chondrules (literature sources; see the Supplementary Materials) range from CAI formation to ~4 Ma, similar to the distribution of our RF model ages. All uncertainties are ±2 SE.

and have faster solid-state magnesium diffusion than the larger RFs (~100 μm). Chondrule ages are thus more readily reset than model $\Delta'^{26}Mg$ isotope ages in RFs. While the internal Al-Mg isochrons in chondrules may constrain the timing of thermal events in the protoplanetary disc, we suggest that they likely do not represent formation ages.

Although RFs formed within at least ~300,000 years of CAIs, they have very different $\Delta'^{17}O$, illustrating that large-scale oxygen isotope heterogeneities were established early in the solar system. This suggests that the process(es) that produced these differences [e.g., photodissociation of CO (*34*, *44*)] was highly efficient or that there was preexisting $\Delta'^{17}O$ heterogeneity in the protosolar molecular cloud that was not homogenized by the time CAI formation began.

Our inference of common $(^{26}Al/^{27}Al)_0$ (at ~5.3×10^{-5}) between CAIs and the major silicate phases from the terrestrial planets—and asteroid-forming reservoirs—supports the underlying assumption of the $^{26}Al \rightarrow ^{26}Mg$ dating system and therefore reaffirms its validity as a widely applicable, high–temporal resolution, early solar system chronometer. Moreover, the remarkable antiquity of RFs, calculated from their $\Delta'^{26}Mg$, demonstrates an important before-unseen consistency with chondrule formation ages determined by the extant ^{207}Pb-^{206}Pb system (*6*), another cornerstone of early solar system chronology.

MATERIALS AND METHODS

We targeted polished sections of two unequilibrated chondrites (primitive meteorites that did not experience high degrees of thermal metamorphism or aqueous alteration on their parent asteroids) in this study: Northwest Africa 4502, a type 3 (*45*) oxidized Vigarano-like carbonaceous chondrite ($CV3_{ox}$), and Felix, a type 3.3 (*46*) Ornans-like carbonaceous chondrite (CO3.3) borrowed from the Natural History Museum, London (identification number: P13341). Candidate grains were identified and imaged using scanning electron microscopy (backscattered electrons and x-ray energy-dispersive spectroscopy) at the University of Bristol (UK), and their in situ chemical composition was measured using electron probe microanalysis (EPMA) at the University of Bristol. Oxygen isotopes were measured in situ via secondary ionization mass spectrometry at CRPG (Nancy, France). Before ex situ magnesium isotope measurements, each RF was excavated from its host section using a newly developed technique that combines laser excavation and microsampling. Magnesium isotope compositions were measured ex situ via multicollector inductively coupled plasma source mass spectrometry (MC-ICP-MS) at the University of Bristol. These measurements were conducted using a modified protocol that allows for small masses of magnesium (<5 μg) to be measured to high precision (typically better than ±3 ppm on $\Delta'^{26}Mg_{DSM\text{-}3}$, ±2 SE). The reader is referred to the Supplementary Materials for the detailed analytical and microsampling protocols.

SUPPLEMENTARY MATERIALS

Supplementary material for this article is available at http://advances.sciencemag.org/cgi/content/full/6/11/eaay9626/DC1

Supplementary Text

Fig. S1. Δ'^{26}Mg evolution models for three major classes of chondritic meteorites.

Fig. S2. Aluminum blank correction models.

Fig. S3. The empirically derived terrestrial oxygen isotope fractionation line.

Fig. S4. Microexcavation of an RF.

Fig. S5. Magnesium isotope measurements of reference solutions.

Fig. S6. Measurements of samples using long measurement times.

Fig. S7. ^{27}Al/^{24}Mg measurements of the JP-1 reference material.

Fig. S8. A summary of false-color K_α x-ray maps of the 13 RFs analyzed in this study.

Fig. S9. Detailed scanning electron microscope image of RF C9 (Felix).

Fig. S10. Detailed scanning electron microscope image of RF C9a (NWA 4502).

Fig. S11. Detailed scanning electron microscope image of RFs C19a and C19b (NWA 4502).

Fig. S12. Detailed scanning electron microscope image of RF C39 (NWA 4502).

Fig. S13. Detailed scanning electron microscope image of RF C4 (NWA 4502).

Fig. S14. Detailed scanning electron microscope image of RF C18 (NWA 4502).

Fig. S15. Detailed scanning electron microscope image of RFs C1a, C1b, and C1c (NWA 4502).

Fig. S16. Detailed scanning electron microscope image of RF C21 (NWA 4502).

Fig. S17. Detailed scanning electron microscope image of RF C34 (NWA 4502).

Fig. S18. Detailed scanning electron microscope image of RF C6 (NWA 4502).

Table S1. A summary of the chemical composition and ^{27}Al/^{24}Mg of RFs measured in situ by EPMA and ex situ by inductively coupled plasma source mass spectrometry.

Table S2. A summary of the oxygen isotope composition of RFs measured in situ by secondary ionization mass spectrometry.

Table S3. A summary of the magnesium isotope composition of RFs measured ex situ by MC-ICP-MS and their associated $\Delta'^{26}Mg_0$ model ages.

References (*49*–*106*)

REFERENCES AND NOTES

1. T. Lee, D. A. Papanastassiou, G. J. Wasserburg, Demonstration of ^{26}Mg excess in Allende and evidence for ^{26}Al. *Geophys. Res. Lett.* **3**, 109–112 (1976).
2. I. D. Hutcheon, R. Hutchison, Evidence from the Semarkona ordinary chondrite for ^{26}Al heating of small planets. *Nature* **337**, 238–241 (1989).
3. S. S. Russell, G. Srinivasan, G. R. Huss, G. J. Wasserburg, G. J. MacPherson, Evidence for widespread ^{26}Al in the solar nebula and constraints for nebula time scales. *Science* **273**, 757–762 (1996).
4. N. Dauphas, M. Chaussidon, A perspective from extinct radionuclides on a young stellar object: The sun and its accretion disk. *Annu. Rev. Earth Planet. Sci.* **39**, 351–386 (2011).
5. Y. Amelin, A. Kaltenbach, T. Iizuka, C. H. Stirling, T. R. Ireland, M. Petaev, S. B. Jacobsen, U–Pb chronology of the Solar System's oldest solids with variable ^{238}U/^{235}U. *Earth Planet. Sci. Lett.* **300**, 343–350 (2010).
6. J. N. Connelly, M. Bizzarro, A. N. Krot, Å. Nordlund, D. Wielandt, M. A. Ivanova, The absolute chronology and thermal processing of solids in the solar protoplanetary disk. *Science* **338**, 651–655 (2012).
7. G. J. MacPherson, A. M. Davis, E. K. Zinner, The distribution of aluminum-26 in the early Solar System—A reappraisal. *Meteoritics* **30**, 365–386 (1995).
8. B. Jacobsen, Q.-z. Yin, F. Moynier, Y. Amelin, A. N. Krot, K. Nagashima, I. D. Hutcheon, H. Palme, ^{26}Al–^{26}Mg and ^{207}Pb–^{206}Pb systematics of Allende CAIs: Canonical solar initial ^{26}Al/^{27}Al ratio reinstated. *Earth Planet. Sci. Lett.* **272**, 353–364 (2008).
9. K. K. Larsen, A. Trinquier, C. Paton, M. Schiller, D. Wielandt, M. A. Ivanova, J. N. Connelly, Å. Nordlund, A. N. Krot, M. Bizzarro, Evidence for magnesium isotope heterogeneity in the solar protoplanetary disk. *Astrophys. J.* **735**, L37 (2011).
10. R. Diehl, H. Halloin, K. Kretschmer, G. G. Lichti, V. Schönfelder, A. W. Strong, A. von Kienlin, W. Wang, P. Jean, J. Knödlseder, J.-P. Roques, G. Weidenspointner, S. Schanne, D. H. Hartmann, C. Winkler, C. Wunderer, Radioactive ^{26}Al from massive stars in the Galaxy. *Nature* **439**, 45–47 (2006).
11. C. Fitoussi, J. Duprat, V. Tatischeff, J. Kiener, F. Naulin, G. Raisbeck, M. Assunção, C. Bourgeois, M. Chabot, A. Coc, C. Engrand, M. Gounelle, F. Hammache, A. Lefebvre, M.-G. Porquet, J.-A. Scarpaci, N. De Séréville, J.-P. Thibaud, F. Yiou, Measurement of the ^{24}Mg(^{3}He,p)^{26}Al cross section: Implication for ^{26}Al production in the early solar system. *Phys. Rev. C* **78**, 044613 (2008).
12. A. N. Krot, K. Makide, K. Nagashima, G. R. Huss, R. C. Ogliore, F. J. Ciesla, L. Yang, E. Hellebrand, E. Gaidos, Heterogeneous distribution of ^{26} Al at the birth of the solar system: Evidence from refractory grains and inclusions. *Meteorit. Planet. Sci.* **47**, 1948–1979 (2012).
13. G. J. Wasserburg, T. Lee, D. A. Papanastassiou, Correlated O and Mg isotopic anomalies in allende inclusions: II. Magnesium. *Geophys. Res. Lett.* **4**, 299–302 (1977).
14. T. R. Ireland, Correlated morphological, chemical, and isotopic characteristics of hibonites from the Murchison carbonaceous chondrite. *Geochim. Cosmochim. Acta* **52**, 2827–2839 (1988).
15. M.-C. Liu, K. D. McKeegan, J. N. Goswami, K. K. Marhas, S. Sahijpal, T. R. Ireland, A. M. Davis, Isotopic records in CM hibonites: Implications for timescales of mixing of isotope reservoirs in the solar nebula. *Geochim. Cosmochim. Acta* **73**, 5051–5079 (2009).
16. R. N. Clayton, L. Grossman, T. K. Mayeda, A component of primitive nuclear composition in carbonaceous meteorites. *Science* **182**, 485–488 (1973).
17. J. L. Birck, An overview of isotopic anomalies in extraterrestrial materials and their nucleosynthetic heritage. *Rev. Mineral. Geochem.* **55**, 25–64 (2004).
18. M. E. Sanborn, J. Wimpenny, C. D. Williams, A. Yamakawa, Y. Amelin, A. J. Irving, Q.-Z. Yin, Carbonaceous achondrites Northwest Africa 6704/6693: Milestones for early Solar System chronology and genealogy. *Geochim. Cosmochim. Acta* **245**, 577–596 (2019).
19. M. Schiller, J. N. Connelly, A. C. Glad, T. Mikouchi, M. Bizzarro, Early accretion of protoplanets inferred from a reduced inner Solar System ^{26}Al inventory. *Earth Planet. Sci. Lett.* **420**, 45–54 (2015).
20. J. Bollard, N. Kawasaki, N. Sakamoto, M. Olsen, S. Itoh, K. Larsen, D. Wielandt, M. Schiller, J. N. Connelly, H. Yurimoto, M. Bizzarro, Combined U-corrected Pb-Pb dating and ^{26}Al-^{26}Mg systematics of individual chondrules – Evidence for a reduced initial abundance of ^{26}Al amongst inner Solar System chondrules. *Geochim. Cosmochim. Acta* **260**, 62–83 (2019).
21. Y. Amelin, P. Koefoed, T. Iizuka, V. A. Fernandes, M. H. Huyskens, Q.-Z. Yin, A. J. Irving, U-Pb, Rb-Sr and Ar-Ar systematics of the ungrouped achondrites Northwest Africa 6704 and Northwest Africa 6693. *Geochim. Cosmochim. Acta* **245**, 628–642 (2019).
22. E. D. Young, A. Galy, The isotope geochemistry and cosmochemistry of Magnesium. *Rev. Mineral. Geochem.* **55**, 197–230 (2004).
23. H. Hiyagon, A. Hashimoto, ^{16}O excesses in olivine inclusions in Yamato-86009 and Murchison chondrites and their relation to CAIs. *Science* **283**, 828–831 (1999).
24. R. K. Mishra, M. Chaussidon, Timing and extent of Mg and Al isotopic homogenization in the early inner Solar System. *Earth Planet. Sci. Lett.* **390**, 318–326 (2014).
25. J. Villeneuve, M. Chaussidon, G. Libourel, Homogeneous distribution of ^{26}Al in the Solar System from the Mg isotopic composition of chondrules. *Science* **325**, 985–988 (2009).
26. S. S. Russell, H. C. Connolly, A. N. Krot, *Chondrules: Records of Protoplanetary Disk Processes* (Cambridge Univ. Press, 2018).
27. A. Pack, H. Yurimoto, H. Palme, Petrographic and oxygen-isotopic study of refractory forsterites from R-chondrite Dar al Gani 013 (R3.5–6), unequilibrated ordinary and carbonaceous chondrites. *Geochim. Cosmochim. Acta* **68**, 1135–1157 (2004).
28. I. M. Steele, Compositions of isolated forsterites in Ornans (C3O). *Geochim. Cosmochim. Acta* **53**, 2069–2079 (1989).
29. R. H. Jones, Petrology and mineralogy of type II, FeO-rich chondrules in Semarkona (LL3.0): Origin by closed-system fractional crystallization, with evidence for supercooling. *Geochim. Cosmochim. Acta* **54**, 1785–1802 (1990).
30. I. M. Steele, J. V. Smith, C. Skirius, Cathodoluminescence zoning and minor elements in forsterites from the Murchison (C2) and Allende (C3V) carbonaceous chondrites. *Nature* **313**, 294–297 (1985).
31. A. Pack, H. Palme, J. M. G. Shelley, Origin of chondritic forsterite grains. *Geochim. Cosmochim. Acta* **69**, 3159–3182 (2005).
32. R. H. Jones, A. J. Schilk, Chemistry, petrology and bulk oxygen isotope compositions of chondrules from the Mokoia CV3 carbonaceous chondrite. *Geochim. Cosmochim. Acta* **73**, 5854–5883 (2009).
33. A. N. Krot, Refractory inclusions in carbonaceous chondrites: Records of early solar system processes. *Meteorit. Planet. Sci.* **54**, 1647–1691 (2019).
34. E. D. Young, Time-dependent oxygen isotopic effects of CO self shielding across the solar protoplanetary disk. *Earth Planet. Sci. Lett.* **262**, 468–483 (2007).
35. A. Trinquier, T. Elliott, D. Ulfbeck, C. Coath, A. N. Krot, M. Bizzarro, Origin of nucleosynthetic isotope heterogeneity in the solar protoplanetary disk. *Science* **324**, 374–376 (2009).
36. E. M. M. E. Van Kooten, D. Wielandt, M. Schiller, K. Nagashima, A. Thomen, K. K. Larsen, M. B. Olsen, Å. Nordlund, A. N. Krot, M. Bizzarro, Isotopic evidence for primordial molecular cloud material in metal-rich carbonaceous chondrites. *Proc. Natl. Acad. Sci. U.S.A.* **113**, 2011–2016 (2016).
37. T.-H. Luu, R. C. Hin, C. D. Coath, T. Elliott, Bulk chondrite variability in mass independent magnesium isotope compositions—Implications for initial solar system ^{26}Al/^{27}Al and the timing of terrestrial accretion. *Earth Planet. Sci. Lett.* **522**, 166–175 (2019).
38. N. T. Kita, Q.-Z. Yin, G. J. MacPherson, T. Ushikubo, B. Jacobsen, K. Nagashima, E. Kurahashi, A. N. Krot, S. B. Jacobsen, ^{26}Al- ^{26}Mg isotope systematics of the first solids in the early solar system. *Meteorit. Planet. Sci.* **48**, 1383–1400 (2013).
39. K. D. McKeegan, M. Chaussidon, F. Robert, Incorporation of short-lived ^{10}Be in a calcium-aluminum-rich inclusion from the allende meteorite. *Science* **289**, 1334–1337 (2000).
40. K. J. Walsh, A. Morbidelli, S. N. Raymond, D. P. O'Brien, A. M. Mandell, A low mass for Mars from Jupiter's early gas-driven migration. *Nature* **475**, 206–209 (2011).

41. G. Libourel, A. N. Krot, L. Tissandier, Role of gas-melt interaction during chondrule formation. *Earth Planet. Sci. Lett.* **251**, 232–240 (2006).
42. J. Bollard, J. N. Connelly, M. J. Whitehouse, E. A. Pringle, L. Bonal, J. K. Jørgensen, Å. Nordlund, F. Moynier, M. Bizzarro, Early formation of planetary building blocks inferred from Pb isotopic ages of chondrules. *Sci. Adv.* **3**, e1700407 (2017).
43. H. C. Connolly Jr., R. H. Jones, Chondrules: The canonical and noncanonical views. *J. Geophys. Res. Planets* **121**, 1885–1899 (2016).
44. J. R. Lyons, E. D. Young, CO self-shielding as the origin of oxygen isotope anomalies in the early solar nebula. *Nature* **435**, 317–320 (2005).
45. W. R. Van Schmus, J. A. Wood, A chemical-petrologic classification for the chondritic meteorites. *Geochim. Cosmochim. Acta* **31**, 747–765 (1967).
46. D. W. Sears, J. N. Grossman, C. L. Melcher, L. M. Ross, A. A. Mills, Measuring metamorphic history of unequilibrated ordinary chondrites. *Nature* **287**, 791–795 (1980).
47. M. Schiller, M. R. Handler, J. A. Baker, High-precision Mg isotopic systematics of bulk chondrites. *Earth Planet. Sci. Lett.* **297**, 165–173 (2010).
48. T. Ushikubo, M. Kimura, N. T. Kita, J. W. Valley, Primordial oxygen isotope reservoirs of the solar nebula recorded in chondrules in Acfer 094 carbonaceous chondrite. *Geochim. Cosmochim. Acta* **90**, 242–264 (2012).
49. H.-W. Chen, J. L. Claydon, T. Elliott, C. D. Coath, Y.-J. Lai, S. S. Russell, Chronology of formation of early solar system solids from bulk Mg isotope analyses of CV3 chondrules. *Geochim. Cosmochim. Acta* **227**, 19–37 (2018).
50. P. Friend, D. C. Hezel, D. Mucerschi, The conditions of chondrule formation, Part II: Open system. *Geochim. Cosmochim. Acta.* **173**, 198–209 (2016).
51. A. N. Krot, M. I. Petaev, S. S. Russell, S. Itoh, T. J. Fagan, H. Yurimoto, L. Chizmadia, M. K. Weisberg, M. Komatsu, A. A. Ulyanov, K. Keil, Amoeboid olivine aggregates and related objects in carbonaceous chondrites: Records of nebular and asteroid processes. *Geochemistry* **64**, 185–239 (2004).
52. N. Sugiura, M. I. Petaev, M. Kimura, A. Miyazaki, H. Hiyagon, Nebular history of amoeboid olivine aggregates. *Meteorit. Planet. Sci.* **44**, 559–572 (2009).
53. R. H. Jones, L. A. Leshin, Y. Guan, Z. D. Sharp, T. Durakiewicz, A. J. Schilk, Oxygen isotope heterogeneity in chondrules from the Mokoia CV3 carbonaceous chondrite. *Geochim. Cosmochim. Acta* **68**, 3423–3438 (2004).
54. N. G. Rudraswami, T. Ushikubo, D. Nakashima, N. T. Kita, Oxygen isotope systematics of chondrules in the Allende CV3 chondrite: High precision ion microprobe studies. *Geochim. Cosmochim. Acta* **75**, 7596–7611 (2011).
55. A. N. Krot, A. Meibom, M. K. Weisberg, K. Keil, The CR chondrite clan: Implications for early solar system processes. *Meteorit. Planet. Sci.* **37**, 1451–1490 (2002).
56. J. Aléon, A. N. Krot, K. D. McKeegan, Calcium–aluminum-rich inclusions and amoeboid olivine aggregates from the CR carbonaceous chondrites. *Meteorit. Planet. Sci.* **37**, 1729–1755 (2002).
57. T. J. Fagan, A. N. Krot, K. Keil, H. Yurimoto, Oxygen isotopic evolution of amoeboid olivine aggregates in the reduced CV3 chondrites Efremovka, Vigarano, and Leoville. *Geochim. Cosmochim. Acta* **68**, 2591–2611 (2004).
58. R. N. Clayton, N. Onuma, L. Grossman, T. K. Mayeda, Distribution of the pre-solar component in Allende and other carbonaceous chondrites. *Earth Planet. Sci. Lett.* **34**, 209–224 (1977).
59. K. Makide, K. Nagashima, A. N. Krot, G. R. Huss, I. D. Hutcheon, A. Bischoff, Oxygen- and magnesium-isotope compositions of calcium–aluminum-rich inclusions from CR2 carbonaceous chondrites. *Geochim. Cosmochim. Acta* **73**, 5018–5050 (2009).
60. N. Kawasaki, S. Itoh, N. Sakamoto, H. Yurimoto, Chronological study of oxygen isotope composition for the solar protoplanetary disk recorded in a fluffy Type A CAI from Vigarano. *Geochim. Cosmochim. Acta* **201**, 83–102 (2017).
61. K. D. McKeegan, A. P. A. Kallio, V. S. Heber, G. Jarzebinski, P. H. Mao, C. D. Coath, T. Kunihiro, R. C. Wiens, J. E. Nordholt, R. W. Moses Jr., D. B. Reisenfeld, A. J. G. Jurewicz, D. S. Burnett, The oxygen isotopic composition of the sun inferred from captured solar wind. *Science* **332**, 1528–1532 (2011).
62. A. Bouvier, M. Wadhwa, The age of the Solar System redefined by the oldest Pb–Pb age of a meteoritic inclusion. *Nat. Geosci.* **3**, 637–641 (2010).
63. N. T. Kita, T. Ushikubo, K. B. Knight, R. A. Mendybaev, A. M. Davis, F. M. Richter, J. H. Fournelle, Internal ^{26}Al–^{26}Mg isotope systematics of a Type B CAI: Remelting of refractory precursor solids. *Geochim. Cosmochim. Acta* **86**, 37–51 (2012).
64. G. J. MacPherson, E. S. Bullock, P. E. Janney, N. T. Kita, T. Ushikubo, A. M. Davis, M. Wadhwa, A. N. Krot, Early solar nebula condensates with canonical, not supracanonical, initial ^{26}Al/^{27}Al ratios. *Astrophys. J. Lett.* **711**, L117 (2010).
65. A. J. Fahey, J. N. Goswami, K. D. McKeegan, E. Zinner, ^{26}Al, ^{244}Pu, ^{50}Ti, REE, and trace element abundances in hibonite grains from CM and CV meteorites. *Geochim. Cosmochim. Acta* **51**, 329–350 (1987).
66. G. J. MacPherson, N. T. Kita, T. Ushikubo, E. S. Bullock, A. M. Davis, Well-resolved variations in the formation ages for Ca–Al-rich inclusions in the early Solar System. *Earth Planet. Sci. Lett.* **331–332**, 43–54 (2012).
67. N. T. Kita, H. Nagahara, S. Togashi, Y. Morishita, A short duration of chondrule formation in the solar nebula: Evidence from ^{26}Al in Semarkona ferromagnesian chondrules. *Geochim. Cosmochim. Acta* **64**, 3913–3922 (2000).
68. H. Yurimoto, J. T. Wasson, Extremely rapid cooling of a carbonaceous-chondrite chondrule containing very ^{16}O-rich olivine and a ^{26}Mg-excess. *Geochim. Cosmochim. Acta* **66**, 4355–4363 (2002).
69. N. Sugiura, A. N. Krot, ^{26}Al-^{26}Mg systematics of Ca-Al-rich inclusions, amoeboid olivine aggregates, and chondrules from the ungrouped carbonaceous chondrite Acfer 094. *Meteorit. Planet. Sci.* **42**, 1183–1195 (2007).
70. N. G. Rudraswami, J. N. Goswami, B. Chattopadhyay, S. K. Sengupta, A. P. Thapliyal, ^{26}Al records in chondrules from unequilibrated ordinary chondrites: II. Duration of chondrule formation and parent body thermal metamorphism. *Earth Planet. Sci. Lett.* **274**, 93–102 (2008).
71. N. G. Rudraswami, J. N. Goswami, ^{26}Al in chondrules from unequilibrated L chondrites: Onset and duration of chondrule formation in the early solar system. *Earth Planet. Sci. Lett.* **257**, 231–244 (2007).
72. K. Nagashima, A. N. Krot, M. Chaussidon, Aluminum-magnesium isotope systematics of chondrules from CR chondrites, in *70th Annual Meteoritical Society Meeting* (2007), p. 5291.
73. K. Nagashima, A. N. Krot, G. R. Huss, ^{26}Al in chondrules from CR carbonaceous chondrites, in *39th Lunar and Planetary Science Conference* (2008), p. 2224.
74. S. Mostefaoui, N. T. Kita, S. Togashi, S. Tachibana, H. Nagahara, Y. Morishita, The relative formation ages of ferromagnesian chondrules inferred from their initial aluminum-26/aluminum-27 ratios. *Meteorit. Planet. Sci.* **37**, 421–438 (2002).
75. R. K. Mishra, J. N. Goswami, S. Tachibana, G. R. Huss, N. G. Rudraswami, ^{60}Fe and ^{26}Al in chondrules from unequilibrated chondrites: Implications for early Solar System processes. *Astrophys. J. Lett.* **714**, L217 (2010).
76. T.-H. Luu, E. D. Young, M. Gounelle, M. Chaussidon, Short time interval for condensation of high-temperature silicates in the solar accretion disk. *Proc. Natl. Acad. Sci. U.S.A.* **112**, 1298–1303 (2015).
77. E. Kurahashi, N. T. Kita, H. Nagahara, Y. Morishita, ^{26}Al–^{26}Mg systematics of chondrules in a primitive CO chondrite. *Geochim. Cosmochim. Acta* **72**, 3865–3882 (2008).
78. T. Kunihiro, A. E. Rubin, K. D. McKeegan, J. T. Wasson, Initial ^{26}Al/^{27}Al in carbonaceous-chondrite chondrules: Too little ^{26}Al to melt asteroids. *Geochim. Cosmochim. Acta* **68**, 2947–2957 (2004).
79. N. T. Kita, S. Tomomura, S. Tachibana, H. Nagahara, S. Mostefaoui, Y. Morishita, Correlation between aluminum-26 ages and bulk Si/Mg ratios of chondrules from LL3.0-3.1 chondrites, in *36th Annual Lunar and Planetary Science Conference* (2005), p. 1750.
80. I. D. Hutcheon, A. N. Krot, A. A. Ulyanov, ^{26}Al in anorthite-rich chondrules in primitive carbonaceous chondrites: Evidence chondrules post-date CAI, in *31st Annual Lunar and Planetary Science Conference* (2000),p. 1896.
81. W. Hsu, G. R. Huss, G. J. Wasserburg, Al-Mg systematics of CAIs, POI, and ferromagnesian chondrules from Ningqiang. *Meteorit. Planet. Sci.* **38**, 35–48 (2003).
82. Y. Amelin, A. N. Krot, I. D. Hutcheon, A. A. Ulyanov, Lead isotopic ages of chondrules and calcium-aluminum-rich inclusions. *Science* **297**, 1678–1683 (2002).
83. G. A. Brennecka, G. Budde, T. Kleine, Uranium isotopic composition and absolute ages of Allende chondrules. *Meteorit. Planet. Sci.* **50**, 1995–2002 (2015).
84. Y. Amelin, A. Krot, Pb isotopic age of the Allende chondrules. *Meteorit. Planet. Sci.* **42**, 1321–1335 (2007).
85. J. N. Connelly, Y. Amelin, A. N. Krot, M. Bizzarro, Chronology of the solar system's oldest solids. *Astrophys. J. Lett.* **675**, L121 (2008).
86. J. N. Connelly, M. Bizzarro, Pb–Pb dating of chondrules from CV chondrites by progressive dissolution. *Chem. Geol.* **259**, 143–151 (2009).
87. J. Bollard, J. N. Connelly, M. Bizzarro, The absolute chronology of the early Solar System revisited, in *77th Annual Meteoritical Society Meeting* (2014), p. 5234.
88. J. Bollard, J. N. Connelly, M. Bizzarro, Pb-Pb dating of individual chondrules from the CB$_a$ chondrite Gujba: Assessment of the impact plume formation model. *Meteorit. Planet. Sci.* **50**, 1197–1216 (2015).
89. P. Vermeesch, On the visualisation of detrital age distributions. *Chem. Geol.* **312**, 190–194 (2012).
90. A. Galy, O. Yoffe, P. E. Janney, R. W. Williams, C. Cloquet, O. Alard, L. Halicz, M. Wadhwa, I. D. Hutcheon, E. Ramon, J. Carignan, Magnesium isotope heterogeneity of the isotopic standard SRM980 and new reference materials for magnesium-isotope-ratio measurements. *J. Anal. At. Spectrom.* **18**, 1352–1356 (2003).
91. T. B. Coplen, Guidelines and recommended terms for expression of stable-isotope-ratio and gas-ratio measurement results. *Rapid Commun. Mass Spectrom.* **25**, 2538–2560 (2011).
92. W. F. McDonougha, S.-s. Sun, The composition of the Earth. *Chem. Geol.* **120**, 223–253 (1995).
93. E. Anders, N. Grevesse, Abundances of the elements: Meteoritic and solar. *Geochim. Cosmochim. Acta* **53**, 197–214 (1989).
94. H. Palme, Chemical abundances in meteorites, in *Cosmic Chemistry*, G. Klare, Ed. (Springer, 1988), vol. 1, pp. 28–51.
95. J. T. Wasson, G. W. Kallemeyn, Compositions of chondrites. *Philos. Trans. R. Soc. Math. Phys. Eng. Sci.* **325**, 535–544 (1988).
96. L. E. Nyquist, T. Kleine, C.-Y. Shih, Y. D. Reese, The distribution of short-lived radioisotopes in the early solar system and the chronology of asteroid accretion, differentiation, and secondary mineralization. *Geochim. Cosmochim. Acta* **73**, 5115–5136 (2009).

97. M. Bizzarro, C. Paton, K. Larsen, M. Schiller, A. Trinquier, D. Ulfbeck, High-precision Mg-isotope measurements of terrestrial and extraterrestrial material by HR-MC-ICPMS—Implications for the relative and absolute Mg-isotope composition of the bulk silicate Earth. *J. Anal. At. Spectrom.* **26**, 565–577 (2011).
98. K. Nishiizumi, Preparation of ^{26}Al AMS standards. *Nucl. Instrum. Methods Phys. Res. B* **223–224**, 388–392 (2004).
99. R. Middleton, J. Klein, G. M. Raisbeck, F. Yiou, Accelerator mass spectrometry with ^{26}Al. *Nucl. Instrum. Methods Phys. Res.* **218**, 430–438 (1983).
100. T. L. Norris, A. J. Gancarz, D. J. Rokop, K. W. Thomas, Half-life of ^{26}Al. *J. Geophys. Res. Solid Earth* **88**, B331–B333 (1983).
101. E. A. Samworth, E. K. Warburton, G. A. Engelbertink, Beta decay of the ^{26}Al ground state. *Phys. Rev. C* **5**, 138–142 (1972).
102. J. H. Thomas, R. L. Rau, R. T. Skelton, R. W. Kavanagh, Half-life of ^{26}Al. *Phys. Rev. C* **30**, 385–387 (1984).
103. A. J. Fahey, J. N. Goswami, K. D. McKeegan, E. K. Zinner, ^{16}O excesses in Murchison and Murray hibonites: A case against a late supernova injection origin of isotopic anomalies in O, Mg, Ca, and Ti. *Astrophys. J.* **323**, L91 (1987).
104. P. Baertschi, Absolute ^{18}O content of standard mean ocean water. *Earth Planet. Sci. Lett.* **31**, 341–344 (1976).
105. B. L. A. Charlier, C. Ginibre, D. Morgan, G. M. Nowell, D. G. Pearson, J. P. Davidson, C. J. Ottley, Methods for the microsampling and high-precision analysis of strontium and rubidium isotopes at single crystal scale for petrological and geochronological applications. *Chem. Geol.* **232**, 114–133 (2006).
106. E. T. Tipper, P. Louvat, F. Capmas, A. Galy, J. Gaillardet, Accuracy of stable Mg and Ca isotope data obtained by MC-ICP-MS using the standard addition method. *Chem. Geol.* **257**, 65–75 (2008).

Acknowledgments: We thank B. Buse and S. Kearns (University of Bristol) for assistance with the EPMA, J. Villeneuve (CRPG-CNRS, Nancy) for assistance with the SIMS, and the Natural History Museum (London) for loaning polished sections of Felix (P13341) and Eagle Station (P11104). We sincerely thank C. M. O. Alexander and two other anonymous reviewers for their thoughtful and thorough comments on an earlier version of this manuscript and R. Kilma for careful and clear editorial handling. **Funding:** This work was funded by the Natural Environment Research Council GW4+ Doctoral Training Partnership (NE/L002434/1), European Research Council Advanced Grant 321209 ISONEB, STFC consolidated grant ST/R000980/1, and Europlanet under EC grant agreement 654208. **Author contributions:** T.G., T.-H.L., and T.E. designed the experiments. T.G. and T.-H.L. conducted oxygen isotope analyses. T.G. conducted sample preparation, petrographic characterization, in situ chemical measurements, and the development and refinement of microsampling techniques. T.-H.L. refined the magnesium chromatography protocol. T.G., T.-H.L., and C.D.C. established magnesium isotope measurement protocols. T.G. and C.D.C. conducted magnesium isotope analyses. All authors participated in the reduction and interpretation of the data. T.G. and T.E. wrote the manuscript with input from coauthors. **Competing interests:** The authors declare that they have no competing interests. **Data and materials availability:** All data needed to evaluate the conclusions in the paper are present in the paper and/or the Supplementary Materials. Additional data related to this paper may be requested from the authors.

Submitted 1 August 2019
Accepted 11 December 2019
Published 11 March 2020
10.1126/sciadv.aay9626

Citation: T. Gregory, T.-H. Luu, C. D. Coath, S. S. Russell, T. Elliott, Primordial formation of major silicates in a protoplanetary disc with homogeneous ^{26}Al/^{27}Al. *Sci. Adv.* **6**, eaay9626 (2020).